Supplementary Information

Unconventional Capacity Increase Kinetics of Chemically Engineered SnO_2 Aerogel Anode toward Long-Term Stable Lithium-Ion Batteries

Sung Mi Jung, [‡a] Dong Won Kim [‡b] and Hyun Young Jung [*b]

[a]*Environmental Fate & Exposure Research Group, Korea Institute of Toxicology, Jinju-si, Gyeongnam 52834, South Korea.* [b]*Department of Energy Engineering, Gyeongnam National University of Science and Technology, Jinju-si, Gyeongnam 52725, South Korea.*

∗ To whom correspondence should be addressed. E-mail: hyjung@gntech.ac.kr

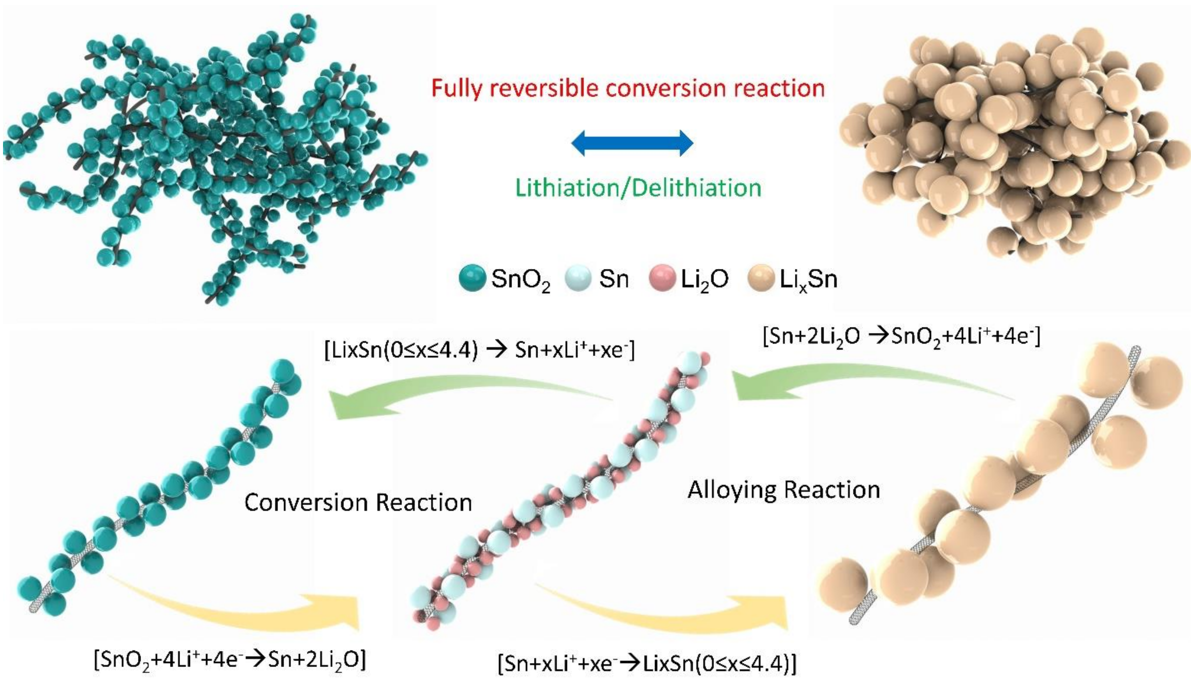

Figure S1. Overall electrochemical reactions between Li-ions and SnO_2 nanoparticles occurring during the lithiation/delithiation processes.

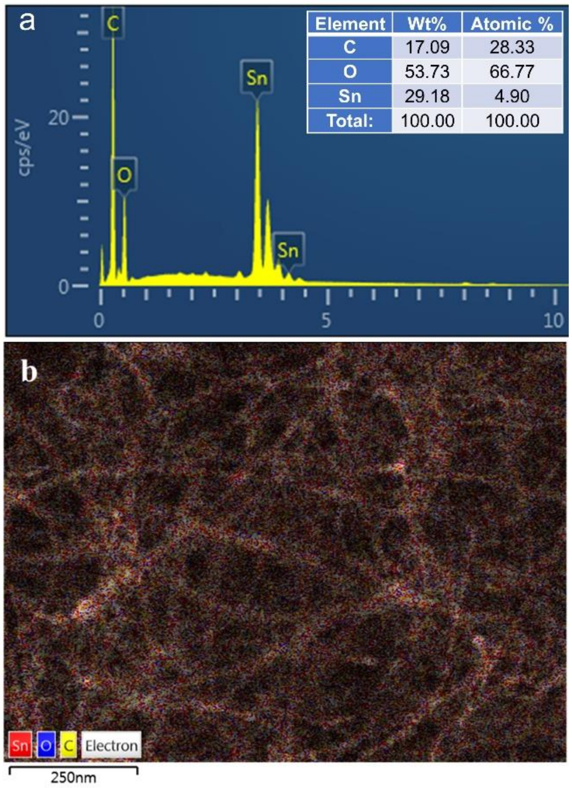

Figure S2. (a) EDS spectrum and (b) element mapping image of the SnO_2 aerogel active material.

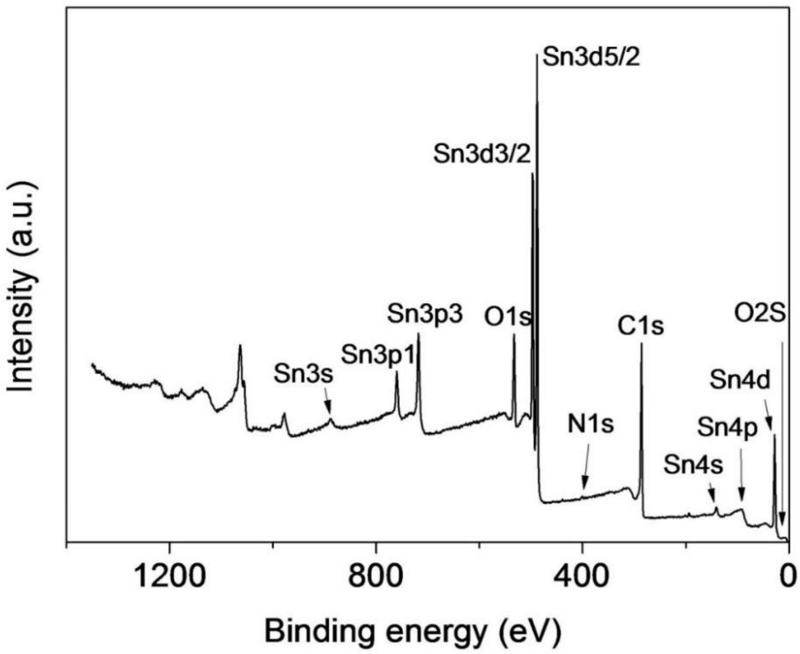

Figure S3. The full XPS spectrum of the SnO_2 aerogel active material.

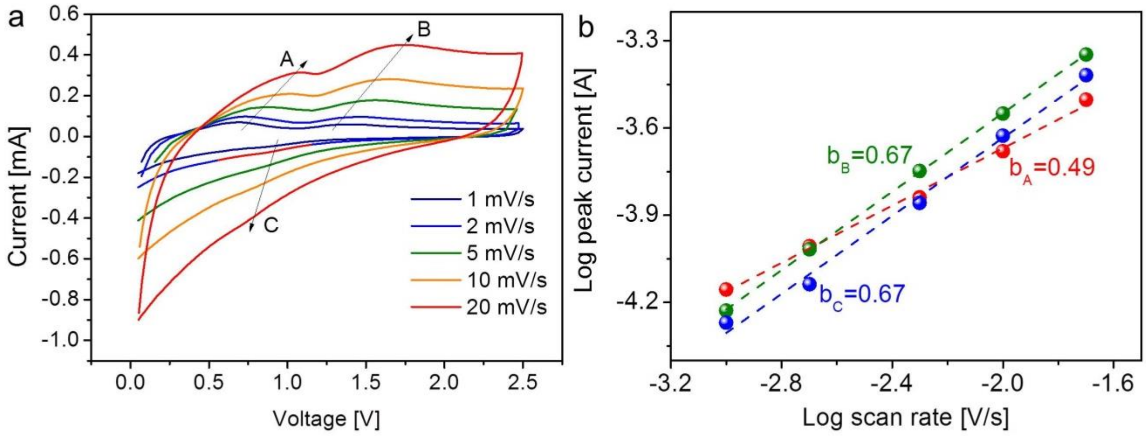

Figure S4. (a) Sequential CV curves with various scan rates of 1, 2, 5, 10, and 10 mV/s. (b) *b*-value at the anodic (A, B) and cathodic (C) peaks in the CV curves.

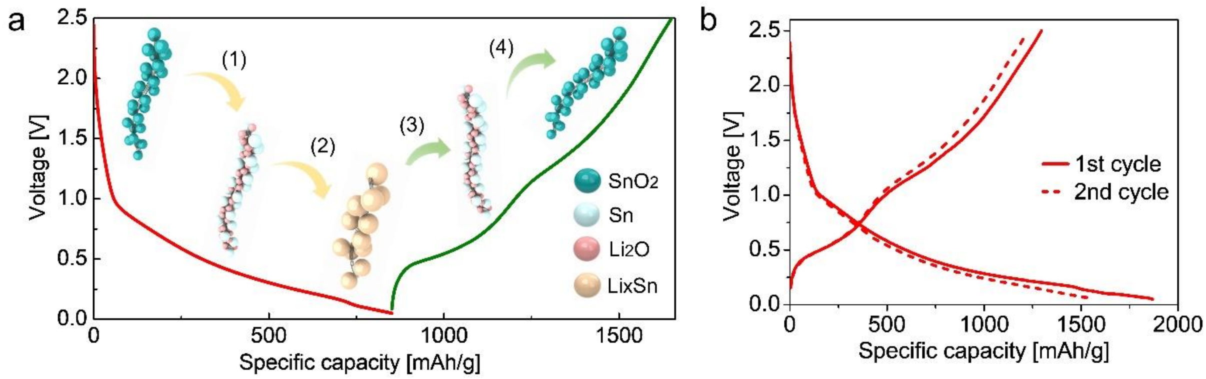

Figure S5. (a) Reaction mechanism according to the lithiation/delithiation cycle, which was representatively measured at a current density of 395 mA g^{-1}. (b) Curves of first and second lithiation/delithiation processes at a current density of 79 mA g^{-1}.

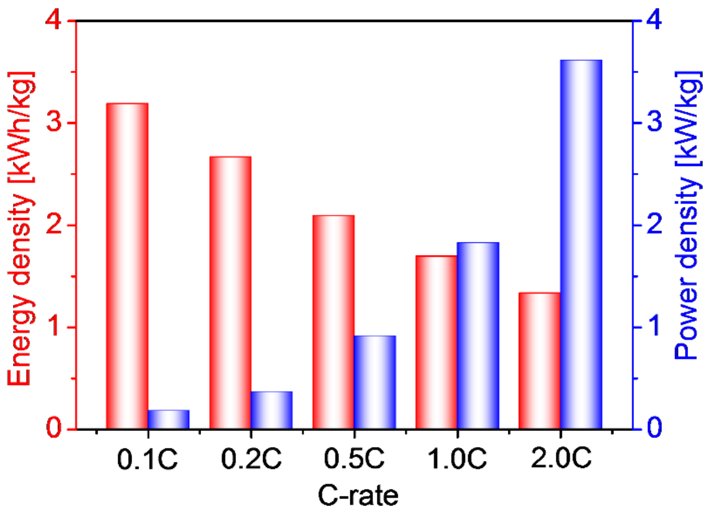

Figure S6. Energy and power densities of the SnO_2 aerogel device extracted from low C-rates (0.1 C to 2 C) of Figures 4a and 4b.

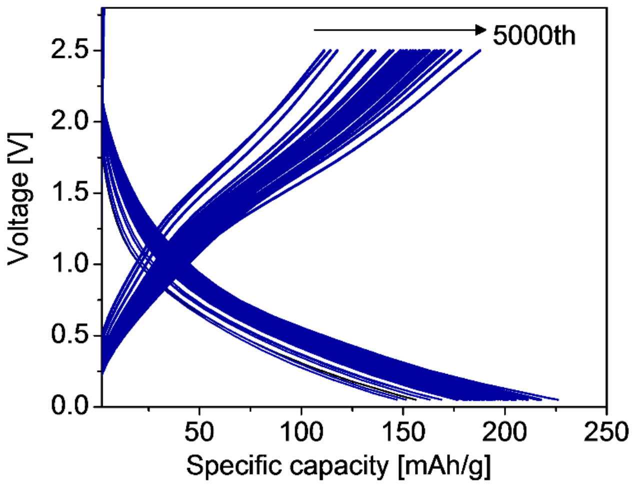

Figure S7. Real time-charge/discharge curves of the SnO_2 aerogel device at 10 C (7900 mA g^{-1}).

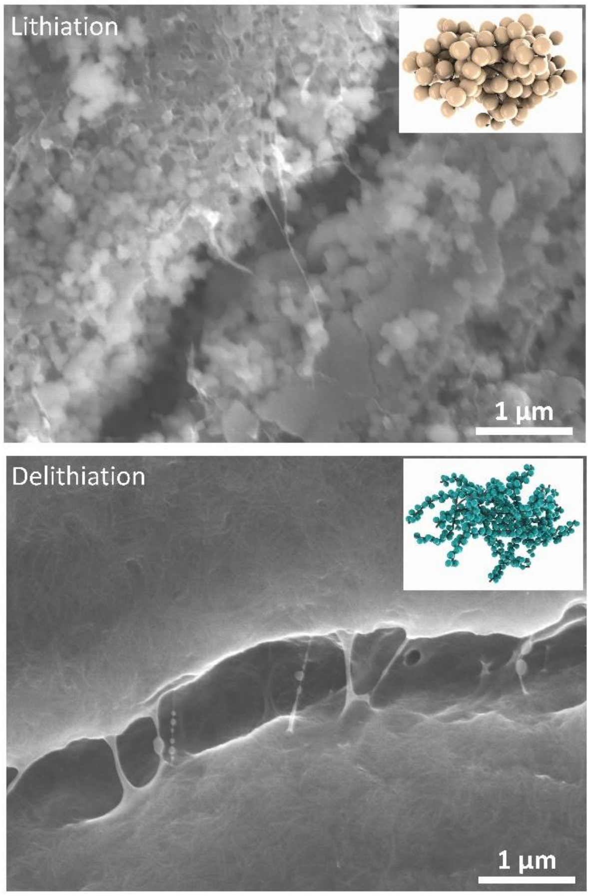

Figure S8. FE-SEM images of the SnO_2 aerogel electrode after 10 cycles at 10 C during lithiation and delithiation processes.

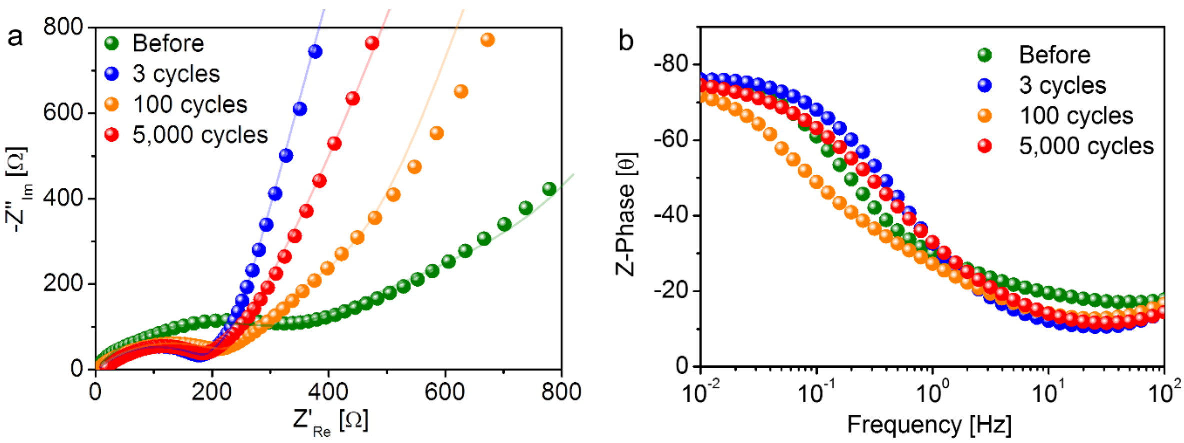

Figure S9. (a) Nyquist plots at the high- and middle frequency region. (b) Z-phase vs. Frequency as a function of cycles.

Table S1. Comparison of discharge capacity and energy density using SnO_2/carbon compound electrodes.

Anode (SnO_2 contents)	OPW[V]	Discharge capacity [mAh/g]	Es[Wh/kg]	Ref.
3D porous SnO_2 aerogel (37wt%)	0.05~2.5	1361, 0.079A/g (5th cycles)	3188	this work
		1919, 0.79A/g (Recovery)	4528	
CNT/Perforated SnO2 (~83.1wt%)	0.001~3.0	1108, 1.5A/g	3323	S1
CNT/c-SnO2 (~72 wt%)	0.01~3.0	1140, 0.05A/g	3409	S2
CNTH/SnO2 (~57.6wt%)	0.01~3.0	1109.5, 0.1A/g	3317	S3
MWCNT/SnO2 (~75wt%)	0.001~2.5	~682, 0.05A/g	1704	S4
MWCNT/SnO2 (~75.5wt%)	0.005~2.5	963, 0.0782A/g	2403	S5
SWNT Paper/SnO2 (~34wt%)	0.01~2.0	~669.52, 0.025A/g	1332	S6
porous-CNT/SnO2 (~64.7wt%)	0.01~3.0	968,0.1A/g	2894	S7
Activated CNT/SnO2 (~65wt%)	0.01~2.5	829.5, 0.2mA/cm2	2037	S8
Gr/CNT/SnO2 (~49.5wt%)	0.01~3.0	947, 0.1A/g	2832	S9
Gr/CNT/SnO2 (~55.3wt%)	0.001~3.0	864, 0.05A/g	2273	S10
Carbon/CNT/SnO2 (~62.39wt%)	0.01~2.5	1572, 0.2A/g	3914	S11
Carbon coated-CNT Sponge/SnO2 (~22.9wt%)	0.01~3.0	~943, 0.1A/g	2820	S12
GF/ SnO2 nanorod array/ PANI (~77wt%)	0.05~3.0	740, 0.1A/g	2183	S13
SGF(Gr Foam)/SnO2 (~45.56wt%)	0.01~3.0	918.1, 0.2A/g	2745	S14
C@SnO2@C HNSs (~54wt%)	0.005~3.0	1123, 0.1A/g	3363	S15
Gr/SnO2 (~67wt%)	0.01~3.0	1025, 0.1A/g	3065	S16

Table S2. Comparison of cycle stability using SnO_2/carbon compound electrodes.

Anode (SnO_2 contents)	OPW[V]	Discharge capacity [mAh/g]	Cyclability [%] and conditions		Ref.
3D porous SnO_2 aerogel (37wt%)	0.05~2.5	1919, 0.79A/g	600	0.79A/g	this work
		224, 7.9A/g	10,000	5.5A/g	
CNT/Perforated SnO_2 (~83.1wt%)	0.001~3.0	1108, 1.5A/g	1000 (>74.5%)	4.0A/g	S1
CNT/c-SnO2 (~72 wt%)	0.01~3.0	1140, 0.05A/g	500 (>72.0%)	1.0A/g	S2
CNTH/SnO2 (~57.6wt%)	0.01~3.0	1109.5, 0.1A/g	100 (>74.2%)	0.2A/g	S3
MWCNT/SnO2 (~75wt%)	0.001~2.5	~682, 0.05A/g	100 (>10.1%)	0.05A/g	S4
MWCNT/SnO2 (~75.5wt%)	0.005~2.5	963, 0.0782A/g	100 (>90%)	3.91A/g	S5
SWNT Paper/SnO2 (~34wt%)	0.01~2.0	~669.52, 0.025A/g	100 (>67.8%)	0.025A/g	S6
porous-CNT/SnO2 (~64.7wt%)	0.01~3.0	968,0.1A/g	500 (>114.1%)	1.0A/g	S7
Activated CNT/SnO2 (~65wt%)	0.01~2.5	829.5, 0.2mA/cm2	50 (>89.7%)	1mA/cm2	S8
Gr/CNT/SnO2 (~49.5wt%)	0.01~3.0	947, 0.1A/g	300(>78.0%)	0.6A/g	S9
Gr/CNT/SnO2 (~55.3wt%)	0.001~3.0	864, 0.05A/g	300(>55.9%)	1.0A/g	S10
Carbon/CNT/SnO2 (~62.39wt%)	0.01~2.5	1572, 0.2A/g	150(>60.7%)	1.0A/g	S11
Carbon coated-CNT Sponge/SnO2 (~22.9wt%)	0.01~3.0	~943, 0.1A/g	100(>90.56%)	0.1A/g	S12
GF/ SnO2 nanorod array/ PANI (~77wt%)	0.05~3.0	740, 0.1A/g	50(>76.8%)	0.5A/g	S13
SGF(Gr Foam)/SnO2 (~45.56wt%)	0.01~3.0	918.1, 0.2A/g	50(>73.9%)	0.2A/g	S14
C@SnO2@C HNSs (~54wt%)	0.005~3.0	1123, 0.1A/g	1000(>92%)	10.0A/g	S15
Gr/SnO2 (~67wt%)	0.01~3.0	1025, 0.1A/g	300(>84%)	0.1A/g	S16
dual carbon shells coated SnO2 hollow nanospheres(41.7%)	0.01~3.0	694, 0.2A/g	300(78.7%)	0.2A/g	S17
dual carbon shells coated SnO2 hollow nanospheres(41.7%)	0.01~3.0	400, 5A/g	10000	5A/g	S17
Sn-SnO2@CNT composite	0.01~3.0	744, 0.5A/g	1000(86%)	0.5A/g	S18

Table S3. EIS fitted parameters of the SnO_2 aerogel cells before cycling and after 3, 100, and 5000 cycles. The fitted typical equivalent circuit model was conducted using ZsimpWin.

Samples	Rs (Ω)	CPE_{SEI}[Y_0, ($Ss^{n1}cm^{-2}$)]	n_1	R_{SEI} (Ω)	CPE_{CT} [Y_0, ($Ss^{n2}cm^{-2}$)]	R_{CT} (Ω)	n_2	W (Y0, $Ss^{0.5}cm^{-2}$)	D_{Li^+}[cm^2s^{-1}]
Fresh	3.3	8.72×10^{-5}	0.68	304.7	3.24×10^{-3}	706.4	0.57	0.562×10^{-2}	2.38×10^{-12}
3 Cycles	3.7	3.63×10^{-4}	0.71	28.5	1.43×10^{-2}	195.2	0.86	1.66×10^{-2}	10.22×10^{-12}
100 Cycles	3.9	4.24×10^{-4}	0.67	34.2	3.22×10^{-2}	208.7	0.81	2.32×10^{-2}	17.22×10^{-12}
5,000 Cycles	3.8	4.03×10^{-4}	0.62	33.5	2.93×10^{-2}	190.2	0.81	2.03×10^{-2}	11.94×10^{-12}

References

[S1] S.H. Choi, J.-H. Lee, Y.C. Kang, *ACS Nano* 2015, **9**, 10173-10185.

[S2] P. Bhattacharya, J.H. Lee, K.K. Kar, H.S. Park, *Chem. Eng. J.* 2019, **369**, 422-431.

[S3] M. Liu, S. Zhang, H. Dong, X. Chen, S. Gao, Y. Sun, W. Li, J. Xu, L. Chen, A. Yuan, W. Li, *ACS Sustainable Chem. Eng.* 2019, **7**, 4195-4203.

[S4] Y. Cheng, J. Huang, H. Qi, L. Cao, J. Yang, Q. Xi, X. Luo, K. Yanagisawa, J. Li, *Small* 2017, **13**, 1700656.

[S5] X. Liu, P. Xu, X. Li, Y. Peng, Z. Le, *J. Mater. Sci.* 2018, **53**, 15621-15630.

[S6] L. Noerochim, J.Z. Wang, S.-L. Chou, D. Wexler, H.-K. Liu, *Carbon* 2012, **50**, 1289-1297.

[S7] W. Zhang, R. Du, C. Zhou, S. Pu, B. Han, K. Xia, Q. Gao, J. Wu, *Mater. Today Energy* 2019, **12**, 303-310.

[S8] H. Zhang, H. Song, X. Chen, J. Zhou, H. Zhang, *Electrochim. Acta* 2012, **59**, 160-167.

[S9] D. Zhou, X. Li, L.-Z. Fan, Y. Deng, *Electrochim. Acta* 2017, **230**, 212-221.

[S10] J. Wang, F. Fang, T. Yuan, J.H. Yang, L. Chen, C. Yao, S.Y. Zheng, D.L. Sun, *ACS Appl. Mater. Interfaces* 2017, **9**, 3544–3553.

[S11] C. Ma, W. Zhang, Y.-S. He, Q. Gong, H. Che, Z.-F.Ma, *Nanoscale* 2016, **8**, 4121-4126.

[S12] B. Luo, T. Qiu, B. Wang, L. Hao, X. Li, A. Cao, L. Zhi, *Nanoscale* 2015, **7**, 20380-20385.

[S13] F. Zhang, C. Yang, X. Gao, S.Chen, Y. Hu, H. Guan, Y. Ma, J. Zhang, H. Zhou, L. Qi, *ACS Appl. Mater. Interfaces* 2017, **9**, 9620-9629.

[S14] R. Tian, Y. Zhang, Z. Chen, H. Duan, B. Xu, Y. Guo, H. Kang, H. Li, H. Liu, *Sci. Rep.* 2016, **6**, 19195.

[S15] J. Qin, N. Zhao, C. Shi, E. Liu, F. He, L. Ma, Q. Li, J. Li, C. He, *J. Mater. Chem. A* 2017, **5**, 10946-10956.

[S16] J. Han, D. Kong, W. Lv, D.-M. Tang, D. Han, C. Zhang, D. Liu, Z. Xiao, X. Zhang, J. Xiao, X. He, F.-C. Hsia, C. Zhang, Y. Tao, D. Golberg, F. Kang, L. Zhi, Q.-H. Yang, *Nat. Commun.* 2018, **9**, 402.

[S17] B. Cao, Z. Liu, C. Xu, J. Huang, H. Fang, Y. Chen, *J. Power Sources* 2019, **414**, 233-241.

[S18] L. Sun, H. Si, Y. Zhang, Y. Shi, K. Wang, J. Liu, Y. Zhang, *J. Power Sources* 2019, **415**, 126-135.